PB-239 997

INFLUENCE OF FIBER CHARACTERISTICS ON PARTICULATE FILTRATION

B. Miller, et al

Textile Research Institute

Prepared for:

National Environmental Research Center

January 1975

DISTRIBUTED BY:

NTIS

National Technical Information Service
U. S. DEPARTMENT OF COMMERCE

TECHNICAL REPORT DATA
(Please read Instructions on the reverse before completing)

1. REPORT NO. EPA-650/2-75-002	2. PB 239 997
4. TITLE AND SUBTITLE: Influence of Fiber Characteristics on Particulate Filtration	5. REPORT DATE: January 1975
	6. PERFORMING ORGANIZATION CODE
7. AUTHOR(S): B. Miller, G.E.R. Lamb, and P. Costanza	8. PERFORMING ORGANIZATION REPORT NO.
9. PERFORMING ORGANIZATION NAME AND ADDRESS: Textile Research Institute, P.O. Box 625, Princeton, NJ 08540	10. PROGRAM ELEMENT NO. 1AB012; ROAP 21ADL-022
	11. CONTRACT/GRANT NO. R-800042
12. SPONSORING AGENCY NAME AND ADDRESS: EPA, Office of Research and Development, NERC-RTP, Control Systems Laboratory, Research Triangle Park, NC 27711	13. TYPE OF REPORT AND PERIOD COVERED Final; 6/72-6/74
	14. SPONSORING AGENCY CODE

15. SUPPLEMENTARY NOTES

APTIC # 1364

16. ABSTRACT

The report gives results of an evaluation of the influence of five fiber parameters (cross-sectional shape, linear density, surface roughness, crimp, and staple length) on the filtration performance of model nonwoven fabrics made from the fibers. Nonwoven fabrics made from 32 polyester fiber samples were used to filter fly-ash particles from a stream of air. Filter performance was assessed by measuring: pressure drop across the filter, collection efficiency, and particle size distribution. Statistically, at 95% confidence: efficiency was improved by using trilobal (rather than round cross-section) fibers with no detrimental effect on drag; efficiency and drag were improved by using crimped (rather than uncrimped) fibers; and efficiency was improved by using 3 (rather than 6) denier fibers, but at the cost of greater drag. These efficiency improvements were especially pronounced for fine particles (approximately 2.5 microns). Non-statistically, except for epitropic fibers with very rough carbon-embedded surfaces, rougher fibers appeared more efficient in removing fine particles. Applying d.c. voltages to 100% non-conducting polyester filters showed considerable increases in efficiency; again, no such effects were seen with polyester filters incorporating 50% epitropic fibers.

17. KEY WORDS AND DOCUMENT ANALYSIS

a. DESCRIPTORS	b. IDENTIFIERS/OPEN ENDED TERMS	c. COSATI Field/Group
Air Pollution	Air Pollution Control	13B
Dust	Stationary Sources	11G
Filtration	Particulates	07D
Fibers	Collection Efficiency	11E
Nonwoven Fabrics		
Particle Size Distribution		14B

18. DISTRIBUTION STATEMENT: Unlimited	19. SECURITY CLASS (This Report): Unclassified	21. NO. OF PAGES: 57
	20. SECURITY CLASS (This page): Unclassified	22. PRICE: 4.25

Reproduced by NATIONAL TECHNICAL INFORMATION SERVICE
US Department of Commerce
Springfield, VA. 22151

EPA Form 2220-1 (9-73)

PRICES SUBJECT TO CHANGE

EPA-650/2-75-002

INFLUENCE OF FIBER CHARACTERISTICS ON PARTICULATE FILTRATION

by

B. Miller, G.E.R. Lamb, and P. Costanza

Textile Research Institute
P.O. Box 625
Princeton, N. J. 08540

Grant No. R-800042
ROAP No. 21ADL-022
Program Element No. 1AB012

EPA Project Officer: J.H. Turner

Control Systems Laboratory
National Environmental Research Center
Research Triangle Park, North Carolina 27711

Prepared for

OFFICE OF RESEARCH AND DEVELOPMENT
U.S. ENVIRONMENTAL PROTECTION AGENCY
WASHINGTON, D.C. 20460

January 1975

iv

EPA REVIEW NOTICE

This report has been reviewed by the National Environmental Research Center - Research Triangle Park, Office of Research and Development, EPA, and approved for publication. Approval does not signify that the contents necessarily reflect the views and policies of the Environmental Protection Agency, nor does mention of trade names or commercial products constitute endorsement or recommendation for use.

This document is available to the public for sale through the National Technical Information Service, Springfield, Virginia 22161.

CONTENTS

		Page
List of Figures		iv
List of Tables		vi
Acknowledgments		vii
Sections		
I	Conclusions	1
II	Recommendations	2
III	Introduction	3
IV	Apparatus	7
V	Filtration Parameters	9
VI	Fabric Filter Formation	11
VII	Experimental Results	18
VIII	EDP Scanning Microscope	33
IX	Epitropic Fibers	35
X	References	42
XI	Glossary	44
XII	Nomenclature	46

FIGURES

No.		Page
1A	Apparatus for measuring filter performance	8
B	Humidity control system	8
2	Scanning electron micrographs of selected fibers used in the main experiment	13
	A. Round, smooth (0.1% TiO_2) (3000X)	
	B. Round, rough (2.0% TiO_2) (3000X)	
	C. Trilobal, smooth (0.1% TiO_2) (1000X)	
	D. Trilobal, rough (2.0% TiO_2) (1000X)	
3	Relationship between air permeability and fabric density	14
4	Relationship between air permeability and latex content	14
5	Half-normal plot for E(1)	20
6	Half-normal plot for E(10)	20
7	Half-normal plot for $\Delta P_e/V$	20
8	Half-normal plot for $\Delta P_f/V$	21
9	Half-normal plot for K	21
10	Half-normal plot for $C_o(10)$	21
11	Half-normal plot for E(2.5μ)	21
12	Three-dimensional plots of the effect of crimp x length on E(10) and $C_o(10)$	25
13	Three-dimensional plot of the effect of shape x length on E(10)	25
14	Three-dimensional plot of the effect of linear density x shape on E(10)	25
15	Efficiency distributions for samples 1 A-D	27
16	Efficiency distributions for samples 2 A-D	27
17	Efficiency distributions for samples 3 A-D	27
18	Efficiency distributions for samples 4 A-D	27

FIGURES (continued)

No.		Page
19	Efficiency distributions for samples 5 A-D	28
20	Efficiency distributions for samples 6 A-D	28
21	Efficiency distributions for samples 7 A-D	28
22	Efficiency distributions for samples 8 A-D	28
23	Scanning electron micrographs of filters 4C and 6A (150X)	30
24	Optical density contour maps of filter samples A. Low density sample #4C (5.5X) B. Low density sample #4A (5.5X) C. High density sample #4C (5.5X) D. High density sample #4A (5.5X)	34
25	Micrograph of epitropic fiber surface (from Ellis, V. S., Reference 13)	36
26	Micrograph of epitropic fiber cross section (from Ellis, V. S., Reference 13)	36
27	Efficiency distribution curves for 100% polyester and for 50% epitropic/50% polyester filter samples	38
28	Diagram of filtration apparatus modification for electrification trials	39
29	Effect on E(1) of high voltage applied to 100% polyester and to 50% epitropic/50% polyester filters	39
30	Effect on E(1) of high voltage applied to 100% polyester (needled) with and without grounding center of sample	41

TABLES

No.		Page
1	Filtration Parameters	10
2	Description of Experimental Fiber Samples	12
3	Fabric Properties of Main Experiment Samples	16
4	Measurements of Filtration Performance Responses of Main Experiment Samples	17
5	Summary of Yates Analysis at 95% Confidence	23
6	Physical Properties of Epitropic/Polyester Filters	38

ACKNOWLEDGEMENTS

The authors wish to express their appreciation to Dr. J. H. Turner of the Environmental Protection Agency for his advice and encouragement throughout the period of this research. The authors also wish to acknowledge the assistance provided by Professor John C. Whitwell and Dr. Charles J. Shimalla with the statistical analyses.

SECTION I

CONCLUSIONS

Of the five fiber parameters whose effects on filtration performance have been studied, three have been shown to have significant effects. Efficiencies are shown to be improved by the use of trilobal rather than round cross-section fibers, 3-denier rather than 6-denier fibers, and crimped rather than uncrimped fibers. Pressure drops are also improved by the use of crimped fibers. The improvement in efficiency found with low linear density fibers is obtained at the cost of a greater pressure drop. Surface roughness appears to have no effect at the levels studied. A nonstatistical examination of the results, however, seems to indicate that rough fibers are more efficient in removing the smallest particles. At the 90% confidence level, longer staple fibers give improved efficiency.

Significant interactions occurred between crimp and length, shape and length, and linear density and shape. These are difficult to interpret but are tentatively attributed to fabric formation effects. Confirmation of this assumption would require measurements of density fluctuations and pore size distributions in webs made from the different fibers.

Particle size analysis of the dust passing through the filters has shown that improvements in overall efficiency are accompanied by even greater improvements in the efficiency at the small particle end of the distribution curve. It follows that studies of these geometric parameters may be useful in developing filters with improved capacity for removing very small particles.

Experiments with filters made from epitropic fibers did not show significant improvements in efficiency resulting from the greater surface roughness of these fibers. It is not established whether the conductivity of these fibers was active in opposing the effect of roughness.

Application of high D. C. voltages to the filter fabrics show important improvements in efficiency with filters made of 100% non-conducting poly(ethylene terephthalate) (PET) fibers. With PET filters incorporating 50% epitropic fibers, the improvement was much smaller.

SECTION II

RECOMMENDATIONS

The results of this study suggest that further work could be profitably undertaken in the following areas:

1. Extension of the measurements of filtration performance over wider ranges of the fiber parameters. Only two levels of each parameter were examined in this study. While these levels were chosen to be within a practical working range for many textile fabrics, the variables were far from the limit of capabilities of fiber technology. In order to obtain optimum performance, it would clearly be useful to have information on the dependence of filtration responses over a wide range of fiber parameters.

2. Changes in fiber geometry appear to affect filtration performance not only through their own interaction with the dust-laden air stream but also through changes in the structure of the nonwoven filter. A study of density fluctuations and pore size distributions as they are affected by fiber geometry should therefore be made in order to gain an estimate of the relative importance of these effects.

3. The short study reported herein on the effects of electric charges applied to the filter fabrics suggests a considerable potential for improving the performance of fabric filters. This might be achieved by relatively simple modifications of existing equipment. Profitable avenues of research would be the application of electrical voltages, to affect, besides the efficiency, also the cleaning of filters. Optimal results would presumably be obtained by combining such improvements with optimization of fiber geometry.

4. The performance of filter bags made of some of the fabrics used in the present work should be evaluated in order to verify that the results obtained with four inch diameter patch filters are valid for full scale application.

SECTION III

INTRODUCTION

Fabric filters have been used in industrial applications for over a century. Originally introduced as a means of recovering valuable products from gas streams, they still perform this service today. Currently, they are being employed more and more for the cleaning of stack gases in order to reduce levels of air pollution. Properly operated bag filters can remove more than 99.9% of the dust from a stream of gas, and will do so less expensively than many other available devices. The first baghouse filters were made of wool or cotton, these being the only fibers available at the time. More recently, synthetic fibers have been used, mainly for their higher temperature resistance, a valuable advantage in many applications.

Filter bags have been made from a variety of fabrics. The most frequently used are woven or felted cloth. The former, as the name implies, is fabric produced by conventional weaving, some weaves such as satin and twill being preferred. Woven fabrics are durable but on a microscopic scale they present inhomogeneities which reduce their effectiveness. The yarns composing a woven fabric tend to be compact bundles of filaments which do not utilize their maximum filtration potential. The spaces between yarns also tend to form voids or at least present a lower density of filaments to the oncoming dust laden air. Felted cloth represents an attempt to eliminate these shortcomings. Woven wool cloth can be felted by agitating in hot water (precisely the same process that must be avoided when washing woolen garments). Shrinkage and fiber rearrangement result in a more compact, more uniform fabric with some of the characteristics of felt, hence the name. Similar structures are made from synthetic non-felting fibers by combining an open scrim (a very open woven cloth) with a loose mat of fibers and consolidating the whole by some compacting process, usually needle punching. The term nonwoven covers any fabric made without recourse to a weaving step. Nonwovens are made by a variety of processes. They are usually formed from a loose mat of fibers which may be a card web or may be laid from air or liquid suspension. The web is then consolidated by needle punching or by bonding with latex, with a thermoplastic binder fiber or by a chemical process.

In a more recent process, "spunbonded" fabrics are made by spinning, drawing and then blowing a continuous filament onto a moving belt. The filaments form a mat which is then bonded by some suitable means. This process is attractive because it is continuous from polymer to fabric. In a different form, melted polymer from an extruder is converted

by an air jet into many fine filaments. These are blown directly onto a moving screen where they form a fabric-like layer which can be further consolidated by heat and pressure.

Almost any one of the fabrics described above can be used for filtering air, but the selection of one or another for commercial filtration purposes has, in the past, usually been dictated by a multitude of considerations among which are durability, dust loading capacity, cleanability, efficiency, drag characteristics and ability to resist blinding.

Until recently, there has been little application of completely nonwoven fabrics (except paper) to filtration uses. Since nonwovens are potentially better filters than woven fabrics, and since they are also cheaper to produce, there is now considerable interest in the development of completely nonwoven filter bags. Such bags have already been shown to give satisfactory performance in extended trials [1]. Other improvements may be possible with nonwoven filters because methods of fabrication allow a greater range of some properties than can be achieved with woven structures. One example of such a property is fabric density which in the case of nonwovens may be controlled by varying the degree of interfiber bonding.

In a nonwoven, single fiber characteristics assume a dominant role, since the effects of weave patterns, yarn twist, weave density, etc., are absent and the single fiber, rather than the yarn, is the filtering element of the structure. Single fibers may affect and control filtration performance through their geometric properties, surface finish, electrical properties, hardness, and other mechanical properties.

The mechanism of capture of a particle by a single fiber has received the attention of many workers, who have examined the role of diameter [2-3], shape [5,6], surface [7,8], modulus [9], and hardness [9], as well as the ambient relative humidity [10] and the electrical charge on the fiber [11]. When a gas stream is passed through a filter medium, there are three basic mechanisms of particle capture: direct interception, inertial deposition, and diffusion. The first occurs with relatively large particles, which collide with the fibers even when carried along the streamlines of the carrier gas. Inertial deposition occurs when the viscous force of the gas is insufficient to keep the particle following the fluid streamline around the obstacle; inertial forces then increase the probability of impact with the obstacle. Deposition by diffusion occurs significantly only at low gas velocities or long path lengths and with particles of the order of 0.1μ and below. Here the Brownian motion of the particle carries it off the streamline and brings about collision with the obstacle. In all cases, it is assumed that the particle adheres to the obstacle on contact.

Dahneke [9], considering the conditions which would lead to a particle bouncing off an obstacle rather than adhering to it, concluded that for maximum capture ability, fibers should have small diameters and be made of material with a low Young's modulus. Reducing fiber diameter has a two-fold influence on the capture of large particles: (a) it lowers the velocity range in which inertial impaction is effective, and (b) it raises the velocity at which the onset of bouncing occurs. Dahneke's treatment focused attention on the changes in the coefficient of restitution due to the work absorbed in flexural deformation resulting from impact. The coefficient of restitution is the ratio of the velocity of the rebounding particle to the velocity of the impinging particle, both at the moment of impact. Dahneke further examined the effect of the depth of indentation of the particle on the obstacle. The greater the depth, the greater the surface-particle potential well. This increases the limiting velocity for rebound and in effect means that soft surfaces make capture easier than hard ones. This agrees with experimental findings of Zimon and Lazarev [7] and is also intuitively acceptable.

The question of obstacle shape was reviewed by Ranz [5] who showed that, in general, the blunter the body, the higher the impaction efficiency. Thus, a ribbon with its flat side facing the oncoming particles is about 46% more efficient than a cylinder of equal width, while a cylinder is more efficient than a ribbon of elliptical cross section with its thin side facing the oncoming stream. More efficient than a ribbon is a recessed collector, presenting a concave surface to the incoming stream. As will be shown, this is supported by the higher efficiences found in the present work with filters made from trilobal fibers.

The possible effects of obstacle surface roughness on capture efficiency appear not to have been extensively studied, probably because of the difficulty of defining roughness and of introducing a roughness parameter into aerodynamic expressions. Leva [8] found no dependence of permeability on the surface roughness of granules composing a filter bed. His observations were made at low flow rates where the Reynolds number was less than 10. It was assumed that roughness is only important to the extent that it determines the onset of turbulence at higher Reynolds numbers ($\sim 10^3$). However, it would be surprising if roughness were to have no effect at all on capture efficiency, especially when the protuberances are of the same order of magnitude as the particles.

The above remarks illustrate the nature of the considerations involved in this study of the role of single fibers in filtration. Although a great deal of theoretical work has been devoted to the various collection mechanisms, practical testing of the theories appears to have been neglected. This may be

because of the assumption that, since a filter actually operates with an accumulation of dust particles on each fiber, the physical properties of the fibers will be insignificant factors. The work presented here was undertaken to test this assumption.

SECTION IV

APPARATUS

As shown in Figure 1, the filtration test apparatus included: (1) humidity and temperature control devices (see 1B for greater detail, (2) a unit for controlled feeding of particulate matter, (3) a test chamber with provisions for convenient placement of a "patch" filter, (4) a sampling filter to capture particles passing through the test filter, (5) a pump mounted on the exhaust end, (6) devices for cleaning of the test filter by shaking and reverse air flow, (7) means for continuous monitoring of the pressure difference across the test filter, and (8) a flow meter located between the pump and the test filter.

A sequence timer was also incorporated in the apparatus. This consisted of a bank of ten microswitches actuated by cams driven by a common shaft. The microswitches were connected to the various valves and motors so that the full cycle, consisting of preset filtering and cleaning periods, was performed automatically and could be repeated as often as desired. In the present study, one cycle consisted of five minutes of filtering followed by two minutes of reverse air cleaning.

These time periods were arbitrarily chosen.

The following operating conditions were kept constant:

Face velocity: 12.4 cm/sec (24.5 ft/min)

Dust loading (material to air ratio): 5.51 g/m^3 (2.4 grains/ft^3)

Volumetric flow rate: 1040 cm^3/sec (2.2 ft^3/min)

Area of filter: 11.07 cm^2 (0.0873/ft^2)

Relative humidity: 30 ± 2% R. H.

Reverse air velocity: 16.3 cm/sec (32 ft/min)

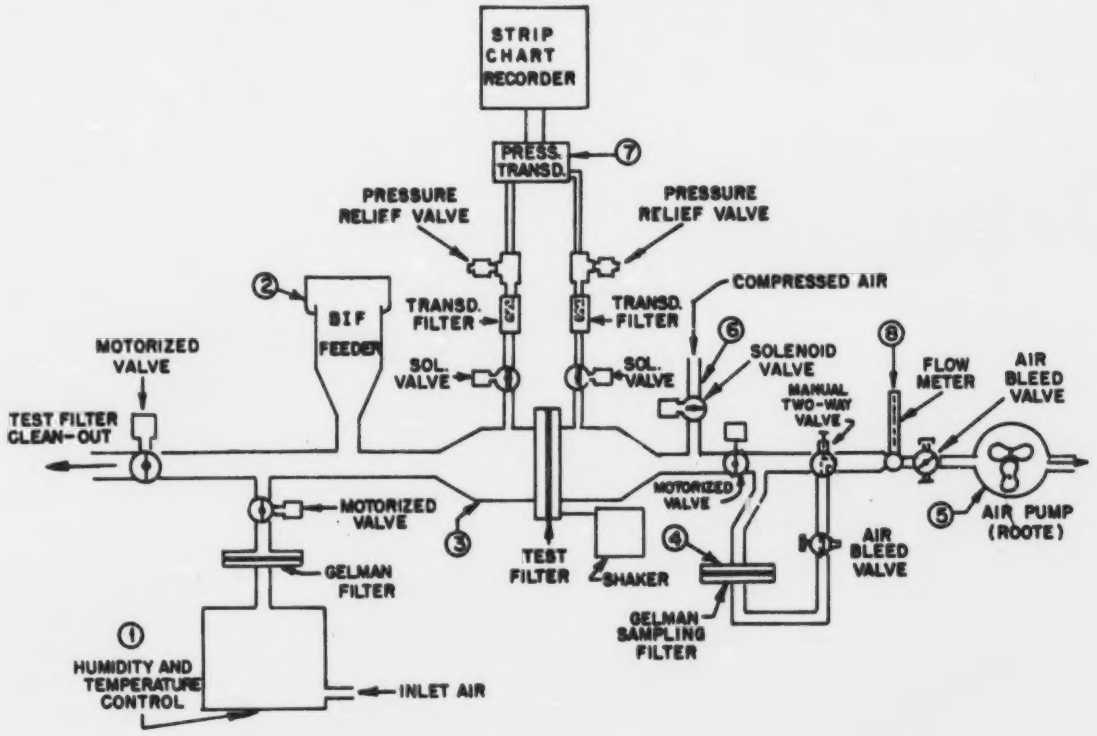

Fig. 1A Apparatus for measuring filter performance.

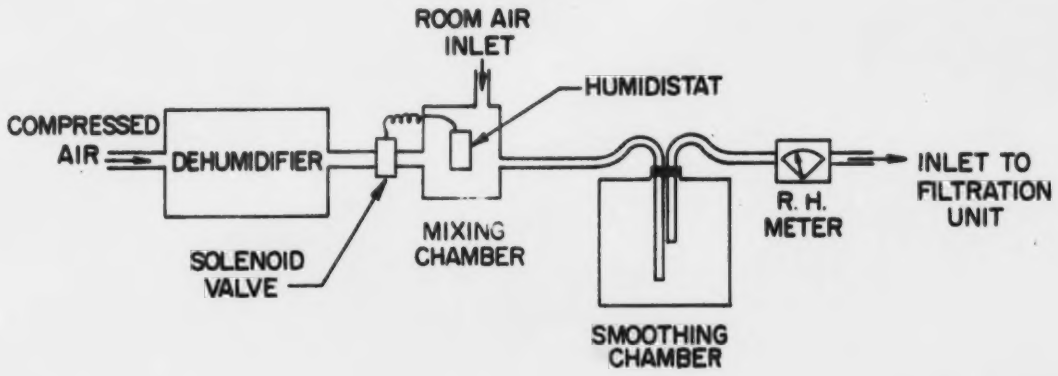

Fig. 1B Humidity control system.

SECTION V

FILTRATION PARAMETERS

In the filtration experiments, the pressure drop was automatically registered on a time base recorder, while mass efficiency was obtained by weighing the amount of fly ash on the main filter and on a sampling filter (0.45μ pore size) through which was passed the full flow of air issuing from the main filter. The fly ash contained particles with diameters up to 40μ. The measurable lower limit was 2.5μ with the instrumentation used. Ten filtering-cleaning cycles were run for each web and efficiencies were measured at the first and tenth cycle.

The filter drag is defined as the pressure drop, ΔP, divided by the face velocity, V. The face velocity is given by

$$V = \frac{\text{Volumetric flow rate through the filter (Q)}}{\text{Area of filter (A)}}$$

The effective drag, $\Delta P_e/V$, is defined as the drag after the filter has been stabilized and is at the point in the filtration cycle where a cake has been established and the change in pressure drop with time becomes a straight line function. In these experiments, it was measured at the beginning of the ninth cycle. The terminal drag, $\Delta P_f/V$, was measured at the end of the ninth filtration cycle, just before cleaning. The specific cake resistance, K, may be written dS/dW, where S is the drag and W is the mass of cake per unit area. It was measured for the tenth cycle.

The outlet concentration, C_o, is the ratio of the mass of dust passed by the filter to the volume of gas passed during a filtration cycle. It may be expressed as $C_o = m_p/Qt_c$, where t_c is the time for one cycle and m_p is the mass passed by the main filter. Outlet concentration was evaluated for the tenth cycle. These parameters are summarized in Table 1.

In addition to the collection of data related to mass efficiency and pressure drop, particle size analysis of fly ash which passed through the main filter was performed using a Coulter Counter. The distribution was then compared to that of the fly ash fed to the main filter.

Table 1

FILTRATION PARAMETERS

1. % Efficiency $= \frac{m_c}{m_c + m_p} \times 100$

2. Effective Drag $= \Delta P_e / V$

   Terminal Drag $= \Delta P_f / V$

   ΔP_e = Initial Pressure Drop

   ΔP_f = Final Pressure Drop

   V = Face Velocity = $\frac{\text{Volumetric Flow Rate, } Q}{\text{Area of Filter, } A}$

3. Specific Cake Resistance, $K = \frac{\Delta P_f/V - \Delta P_e/V}{m_c/A}$

4. Outlet Concentration, $C_o = m_p / Qt_c$

SECTION VI

FABRIC FILTER FORMATION

Fabrics were made from a set of 32 samples of polyester fiber in which two levels each of linear density, cross-sectional shape, surface roughness - obtained by varying titanium dioxide (TiO_2) content - crimp, and staple length were represented. The samples and their code numbers are shown in Table 2. Some of the fiber characteristics are illustrated in the scanning electron micrographs shown in Figure 2.

Various methods of forming the filter fabrics were considered, including needle punching, bonding with low-melting fibers, and bonding with latex. Needle punching was rejected because of the difficulty in maintaining the same fabric density for all fibers. Figure 3 shows the strong dependence of air permeability on fabric density, and illustrates the need for avoiding density variations from sample to sample. Some fabrics were made with low-melting binder fibers, but it was difficult to obtain a good dispersion of these fibers among the base polyester fibers. Latex bonding was finally adopted as the most suitable method.

The problem of different fibers picking up different amounts of latex was examined. The effect of latex content on air permeability was investigated in a separate trial in which the base fiber was kept constant (3 den, 1.5-inch, round, crimped polyester). The filter fabrics used in this trial were formed from cross-laid card webs which were dipped in latex, dried, and consolidated by heating under pressure. The samples were allowed to vary considerably in area density (oz/yd^2) and in percentage latex add-on. (Although it is EPA's policy to use metric units in documents it produces, areadensity [or "weight"] is expressed in non-metric units in this document for the convenience of readers accustomed to textile common usage. The reader may use the conversion factor 1 $oz/yd^2 \equiv 33.91\ g/m^2$.) The latex used, designated Resyn 25-2853, and supplied by the National Starch Company, contained 45% vinyl acetate-acrylic copolymer solids.

The results of air permeability measurements are shown in Figure 4. These are expressed as air permeability (yd/min) multiplied by bulk density (oz/yd^3) and area density or weight (oz/yd^2). The normalized values plotted in Figure 4 are intended to eliminate the effects of density variations as well as those due to any variations in weight. The normalized values thus should reflect only the presence of the latex polymer, which, since it must intrude on the pores in the structure, should cause a decline in air permeability with increasing add-on. This is confirmed by the results shown in

Table 2

DESCRIPTION OF EXPERIMENTAL FIBER SAMPLES

Sample Batch Code	TiO Content (%)	Shape of Cross Section	Linear Density (den)	Crimp Frequency (no./in.)	Nominal Staple Length (in.)
1A	0.1	round	3.0	11-12	3
1B	0.1	round	3.0	11-12	6
1C	0.1	round	3.0	none	3
1D	0.1	round	3.0	none	6
2A	2.0	round	2.7	11-12	3
2B	2.0	round	2.7	11-12	6
2C	2.0	round	2.7	none	3
1D	2.0	round	2.7	none	6
3A	0.1	round	5.9	11-12	3
3B	0.1	round	5.9	11-12	6
3C	0.1	round	5.6	none	3
3D	0.1	round	5.7	none	6
4A	2.0	round	6.6	9-10	3
4B	2.0	round	6.6	9-10	6
4C	2.0	round	6.6	none	3
4D	2.0	round	6.6	none	6
5A	0.1	trilobal	3.2	11-12	3
5B	0.1	trilobal	3.2	11-12	6
5C	0.1	trilobal	3.2	none	3
5D	0.1	trilobal	3.2	none	6
6A	2.0	trilobal	3.3	11-12	3
6B	2.0	trilobal	3.2	11-12	6
6C	2.0	trilobal	3.2	none	3
6D	2.0	trilobal	3.2	none	6
7A	0.1	trilobal	6.2	11-12	3
7B	0.1	trilobal	6.2	11-12	6
7C	0.1	trilobal	6.2	none	3
7D	0.1	trilobal	6.2	none	6
8A	2.0	trilobal	5.7	11-12	3
8B	2.0	trilobal	5.7	11-12	6
8C	2.0	trilobal	5.7	none	3
8D	2.0	trilobal	5.7	none	6

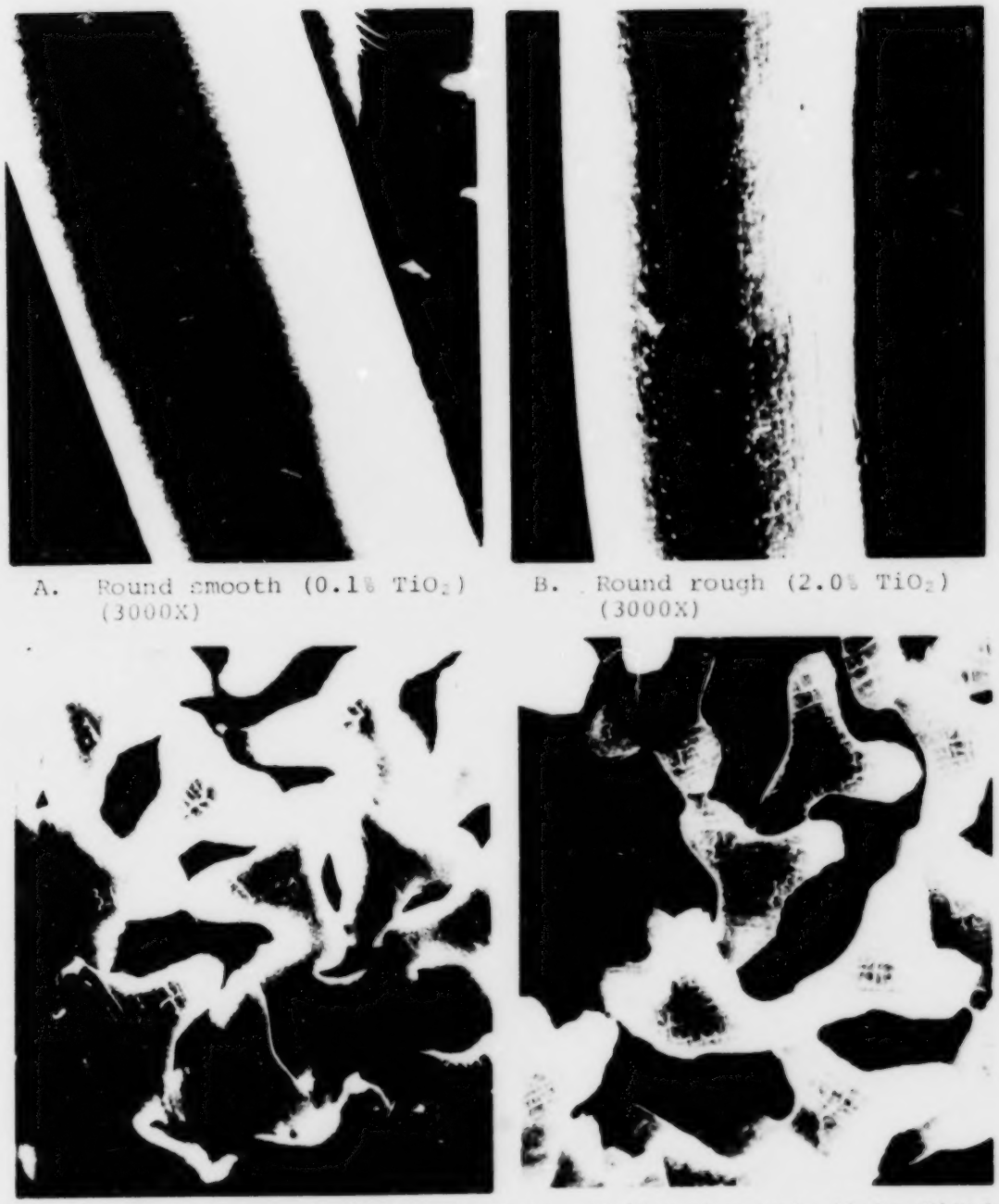

A. Round smooth (0.1% TiO_2) (3000X)

B. Round rough (2.0% TiO_2) (3000X)

C. Trilobal smooth (0.1% TiO_2) (1000X)

D. Trilobal rough (2.0% TiO_2) (1000X)

Fig. 2 Scanning electron micrographs of selected fibers used in the main experiment.

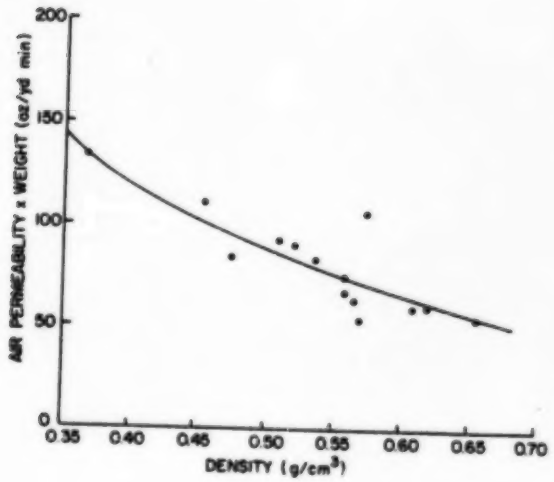

Fig. 3 Relationship between air permeability and fabric density.

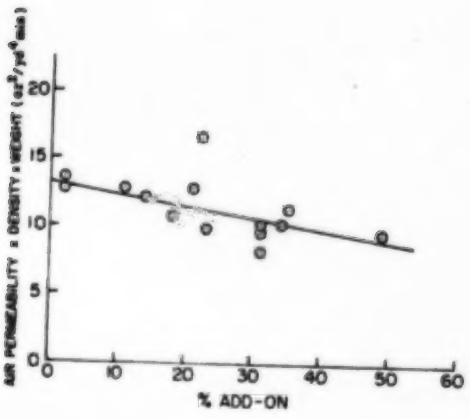

Fig. 4 Relationship between air permeability and latex content.

Figure 4 for a wide range of latex add-on. In the main experment, latex add-on was maintained around 5%. Figure 4 shows that the changes in permeability corresponding to small fluctuations in binder content within this working range can be considered negligible.

Fabric density has a greater effect on air permeability than latex add-on. The need for maintaining constant density in filter fabrics is illustrated by the air permeability data in a somewhat different form (Figure 3). Here air permeability is normalized only for weight and plotted as a function of density. It can be seen that a relatively rapid increase occurs with decreasing density.

All filter webs were made from card webs cross laid in four alternate layers at right angles to one another. Pieces, 5 inches square, were cut from these and their weight adjusted to three grams (corresponding to approximately 5.5 oz/yd^2). These pieces were then immersed in a latex bath, squeeze-rolled four times, and allowed to dry overnight. They were then pressed between Teflon® sheets at 135°C for one minute.

Since the main purpose of this study was to measure the effects of fiber parameters, it was clearly important to minimize the influence of fabric construction. To this purpose, formation pressures were adjusted so as to produce nearly constant fabric densities for all samples. Measured percentages of latex add-on and fabric densities for all the samples in the main experiment are listed in Table 3.

Although efforts were made to keep add-ons, thicknesses and weights within a narrow range, some fluctuations occurred, as shown in the table. Correlation coefficients calculated between these values and the outlet concentrations listed in Table 4 were found to be less than 0.1 and therefore insignificant. Correlation coefficients with respect to terminal drag were slightly higher. However, even the highest (0.335 for percent add-on) was low enough to indicate negligible effect.

Table 3

FABRIC PROPERTIES OF MAIN EXPERIMENT SAMPLES

	% Add-on	Density (g/cm^3)	Weight (oz/yd^2)	Thickness (in.)
1A	4.29	0.213	5.57	0.035
2A	3.69	0.228	5.44	0.032
3A	3.71	0.217	5.58	0.034
4A	3.51	0.208	5.44	0.035
5A	3.19	0.207	5.48	0.035
6A	2.26	0.210	5.52	0.035
7A	2.75	0.229	5.52	0.032
8A	2.79	0.201	5.55	0.037
1C	3.68	0.200	5.51	0.037
2C	3.36	0.213	5.63	0.035
3C	4.56	0.220	5.57	0.034
4C	3.93	0.202	5.62	0.037
5C	6.39	0.223	4.99	0.030
6C	5.18	0.200	5.42	0.036
7C	6.60	0.204	5.40	0.035
8C	5.17	0.209	6.40	0.041
1B	4.82	0.204	6.16	0.040
2B	4.46	0.231	6.19	0.036
3B	4.71	0.223	6.14	0.037
4B	4.31	0.238	5.85	0.033
5B	5.90	0.234	6.01	0.034
6B	5.46	0.224	5.94	0.035
7B	5.43	0.202	5.92	0.039
8B	5.62	0.213	5.83	0.036
1D	4.01	0.230	6.15	0.036
2D	5.24	0.227	6.00	0.035
3D	4.27	0.235	5.98	0.034
4D	4.57	0.226	6.04	0.036
5D	5.71	0.204	5.78	0.038
6D	6.28	0.224	5.85	0.035
7D	5.40	0.227	6.05	0.035
8D	5.12	0.229	5.98	0.035

Table 4

MEASUREMENTS OF FILTRATION PERFORMANCE RESPONSES OF MAIN EXPERIMENT SAMPLES

	E(1) (%)	E(10) (%)	$\Delta P_e/V$ (dyn sec/cm^3)	$\Delta P_f/V$ (dyn sec/cm^3)	K (dyn sec/g cm)	$C_o(10)$ (g/m^3)	E(10)(2.5μ) (%)
1A	99.8	97.8	174	786	3.49	0.69×10^{-7}	93.0
2A	99.6	99.6	195	563	3.46	0.10	97.0
3A	99.1	81.3	160	452	1.28	5.63	0
4A	99.1	76.9	153	320	1.00	7.63	0
5A	99.5	94.6	181	452	2.47	1.04	58.0
6A	99.9	99.9	49	139	2.21	0.03	99.0
7A	98.0	98.2	139	348	2.03	0.28	68.0
8A	97.2	98.8	83	243	1.20	0.45	90.0
1C	99.6	69.0	292	765	2.82	15.63	0
2C	99.7	87.5	389	1377	4.27	6.28	67.0
3C	98.5	70.7	195	522	2.10	12.40	0
4C	98.3	75.9	181	431	1.70	9.86	0
5C	99.8	95.3	195	1064	3.92	1.74	89.0
6C	99.9	99.2	160	835	5.39	0.24	94.5
7C	98.9	84.1	195	522	2.07	6.63	56.0
8C	98.3	89.7	209	626	2.25	3.89	79.5
1B	99.6	97.9	160	542	3.19	0.87	72.5
2B	96.5	97.8	125	512	3.00	0.87	72.0
3B	98.1	81.4	125	431	1.66	15.48	0
4B	98.3	81.0	160	494	2.49	10.36	0
5B	99.4	98.4	160	800	5.19	0.63	79.0
6B	99.6	98.6	146	849	5.33	0.56	86.8
7B	98.9	91.7	125	362	1.91	3.53	0
8B	97.6	94.1	111	327	1.24	2.34	31.6
1D	99.1	93.1	195	85[illegible]	4.99	2.94	10.0
2D	99.7	99.4	139	751	4.74	0.24	94.0
3D	98.5	85.0	153	591	2.67	6.80	0
4D	97.7	82.3	174	584	2.96	7.42	0
5D	98.9	99.2	146	542	2.48	0.32	84.8
6D	99.7	99.3	174	1008	5.85	0.28	90.0
7D	98.8	90.8	132	459	2.48	3.97	10.7
8D	98.6	88.9	137	403	1.92	4.96	0

SECTION VII

EXPERIMENTAL RESULTS

A. Statistical Analysis of Filtration Data

Determination of efficiency and drag characteristics were made in the manner described above. The results were examined by using the so-called Yates algorithm, a statistical analysis which provides a quantitative assessment of the relative significance of each fiber variable on each filtration parameter, and, in addition, supplies estimates of interactions between variables.

The purpose of the standard Yates method [12] is to determine the effects of a number (k) of variables (X_i) upon a response. This is accomplished by estimating the coefficients of the following equation, which is a model of the system:

$$Y_e = c_o + \sum_{i=1}^{k} c_i X_i + \sum_{i>j}^{k} c_{ij} X_i X_j + \sum_{i>j>\ell}^{k} c_{ij\ell} X_i X_j X_\ell + \ldots$$

where Y_e is the estimated value of the response Y, c_o is the zero-order coefficient, c_i are the first-order coefficients, c_{ij} and $c_{ij\ell}$ are the second and third-order coefficients, and so on. The method yields k first-order effects (main effects), $k(k-1)/2$ second-order effects (two-factor interactions), $k(k-1)(k-2)/2$ three-factor interactions, and so on. This method is applicable only when there are 2^k observations (k an integer) as in the present case.

The significance of each coefficient may be determined by means of a half-normal plot. To prepare such a plot, the coefficients are listed in order of increasing absolute value and assigned rank numbers (from 1 to 31 for 2^5 factorial). The absolute values of the coefficients are then plotted on a linear ordinate scale. The values plotted on the abscissa, which is a probability scale, are given by

$$50 + \frac{50}{N}\left(n - \frac{1}{2}\right)$$

where N is the total number of coefficients (31 for 2^5 factorial), and n is the rank number. The origin of the plot occurs at the 50% point, which is the reason it is called half-normal. On such a plot, most of the points will fall on a straight line. However, if a coefficient is large enough, it may deviate from the line, and the extent of the deviation is a measure of its significance. A quantitative estimate of the significance may be obtained by plotting "guardrails." A

guardrail is drawn from the point where the line crosses 84.2% probability to a point obtained as follows: (1) Multiply the ordinate value at 84.2% probability by a number that depends on the confidence level desired. In this analysis, the value of 0.94 corresponding to the 95% confidence level was used. (2) Add the product to the ordinate value corresponding to the highest rank number (99.2% probability for 2 factorial). Guardrails are shown as dashed lines in Figures 5-11. Points lying above these are accepted as representing nonzero effects, and are accented and labeled in Figures 5-11. Points lying above the guardrail and having the highest Yates coefficients carry the greatest significance. As the coefficients decrease, on point will fall below the guardrail. All points with coefficients lower than this one are not significant even though some may fall above the guardrail.

The above method was applied to the data shown in Table 4. Inspection of this table shows that in most cases tenth-cycle efficiency E(10) is lower than first-cycle efficiency E(1). This is contrary to normal experience in baghouse operation, where efficiency gradually improves with increased dust loading. This effect is due to the high face velocity used in the present study. The 24.5 ft/min velocity is almost an order of magnitude greater than those commonly employed in baghouses (3-4 ft/min). Under these conditions, a greater degree of seepage occurs. These severe conditions were chosen to magnify differences in performance between fabrics.

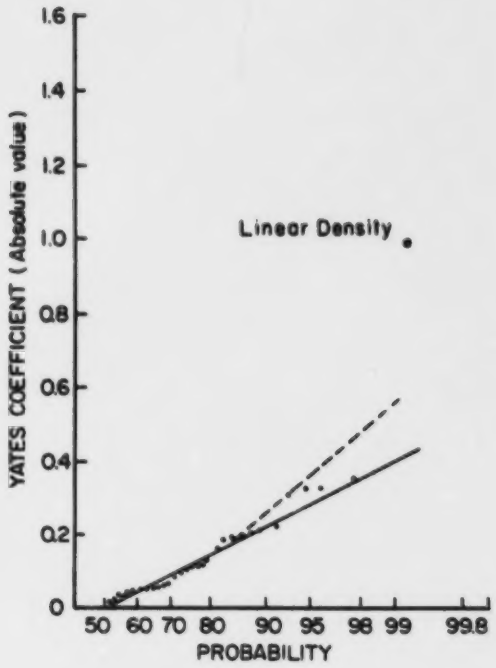

Fig. 5 Half-normal plot for E(1).

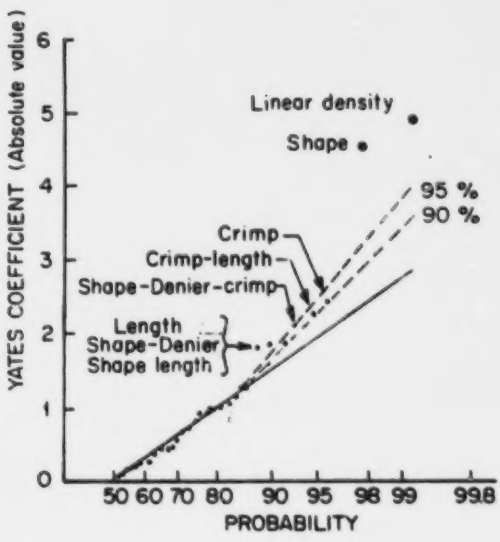

Fig. 6 Half-normal plot for E(10).

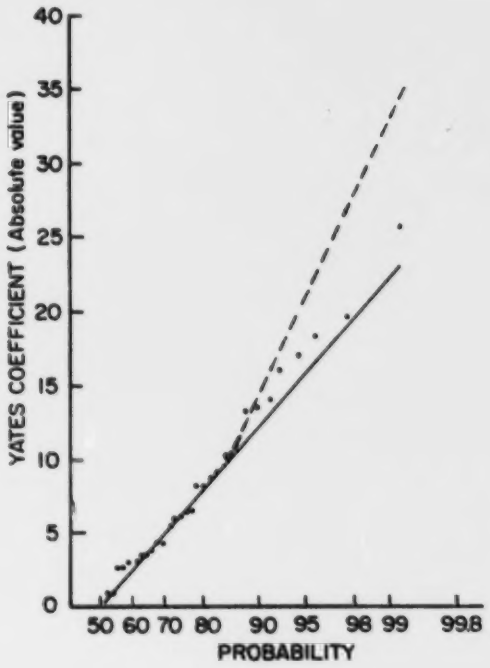

Fig. 7 Half-normal plot for $\Delta P_e/V$.

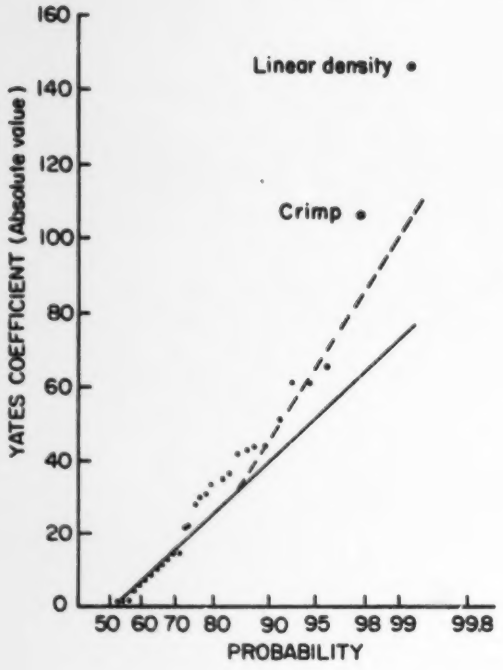

Fig. 8 Half-normal plot for $\Delta P_f/V$.

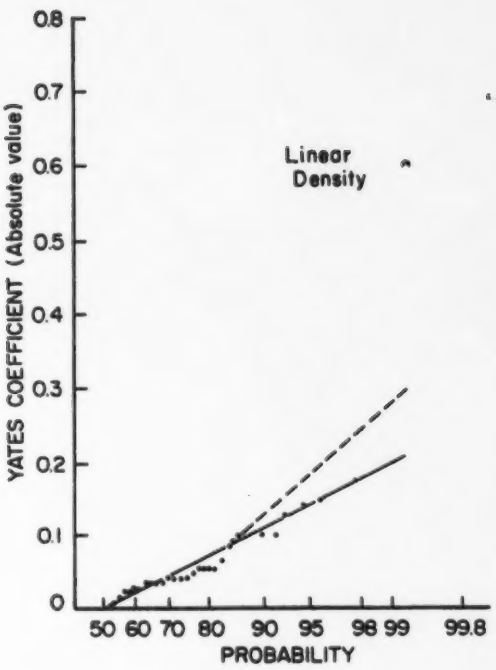

Fig. 9 Half-normal plot for K.

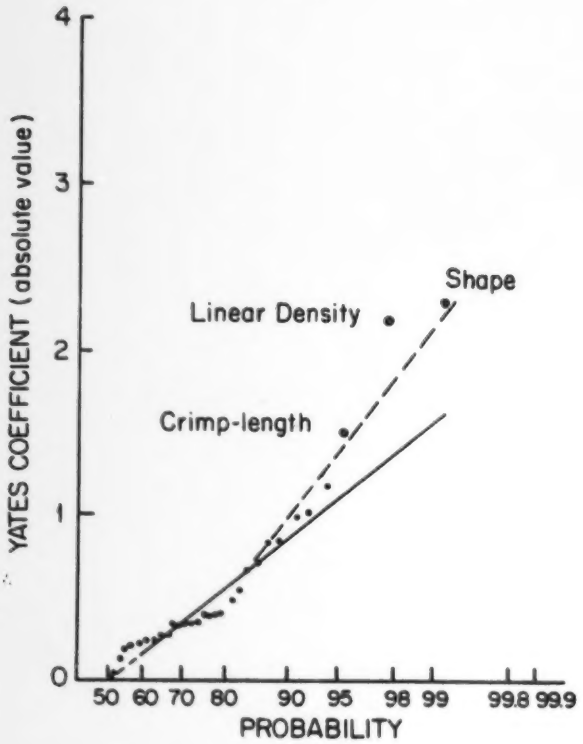

Fig. 10 Half-normal plot for $C_o(10)$.

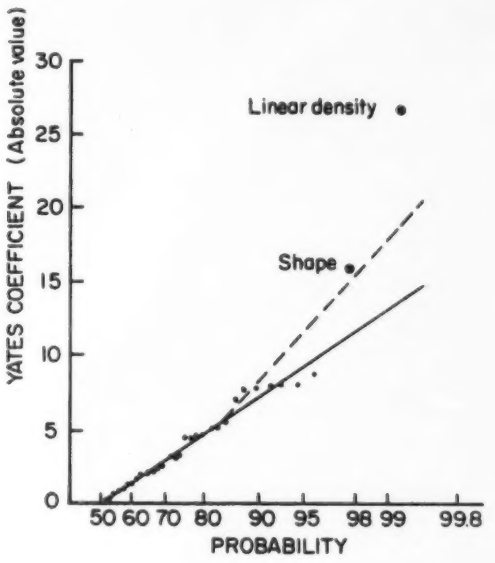

Fig. 11 Half-normal plot for E(2.5μ)

In Table 4 the six dependent variables or responses were: efficiency in the first cycle E(1), efficiency in the tenth cycle E(10), outlet concentration in the tenth cycle $C_o(10)$, effective drag $\Delta P_e/V$, terminal drag $\Delta P_f/V$, and specific cake resistance K. For each of these the effects of the five independent variables were determined by the standard Yates algorithm. The half-normal plots are shown in Figures 5-10, and some of the results of this analysis are given in Table 5, which contains only significant first order effects.

The values shown in the table represent the average response associated with the variable level. For example, the efficiency at the tenth cycle, E(10), improves from 86.0 to 95.0% if the filter is made of trilobal rather than round fibers. The absence of a number indicates no effect.

The following conclusions may be drawn from the 95% confidence level data in the table:

1. Cross-sectional shape: Use of trilobal rather than round fibers improves efficiency with no detrimental effect on drag.

2. Surface roughness: No effect at the levels examined.

3. Linear density: Use of 3-denier rather than 6-denier fibers improves the efficiency but at the cost of increased drag.

4. Crimp level: Use of crimped rather than uncrimped fibers improves drag characteristics.

5. Fiber length: No effect at the levels examined.

In addition to the above effects, Figure 10 indicates that a significant crimp-length interaction occurred with the $C_o(10)$ response at the 95% confidence level. It should be noted that neither crimp nor length alone have significant effects on $C_o(10)$ or on E(10) at this level. To understand this interaction, the graphical presentation shown in Figure 12 was used. The presence of an interaction is indicated when a response depends on two or more variables simultaneously. Such dependence can be represented, as shown, by a surface in a three-dimensional plot for a two-factor interaction. In the original data analysis, an implicit though unstated assumption was that relationships between variables and responses were linear. The plot in Figure 12 illustrates that this is highly unlikely. Also, it is not possible to determine the true shape of the surface from only the four available points. From this graph it can be seen that for short fibers the presence of crimp reduces the outlet concentration considerably, but not for long fibers. Also it can be seen that for uncrimped fibers greater

Table 5

SUMMARY OF YATES ANALYSIS AT 95% CONFIDENCE (32 POINT EXPERIMENT)

	Shape		Roughness		Linear Density		Crimp Level		Fiber Length	
	Round	Trilobal	Smooth	Rough	3 den	6 den	0	12 cpi	3 in.	6 in.
E(1) (%)					99.6	98.4				
E(10) (%)	86.0	95.0			95.4	85.6	88.1	93.0*	88.6	92.4*
$\Delta P_e/V$ (dyn sec/cm^3)										
$\Delta P_f/V$					740	444	708	476		
K (dyn sec/g cm)					3.93	1.94				
$C_o(10)$ (g/m^3)	0.645	0.193			0.203	0.622				
E(2.5μ) (%)	32.0	64.0			73.0	21.0				

*90% Confidence

length produces greater efficiency. The reverse is true for crimped fibers. Therefore, both crimp and length are important parameters but their effect is not linear over the entire 32 point experiment.

Although the 90% confidence level is generally not considered in a 2^5 factorial, for the case of E(10) it is interesting to examine effects at this level. First of all, among these effects are crimp and length alone. Imparting crimp to fibers improves E(10) overall from 88.1 to 93.0%. Increasing fiber length from 3 to 6 inches produces an overall improvement in E(10) from 88.6% to 92.4%. At the 90% confidence level, the crimp-length interaction also appears as represented in Figure 12. The plot is similar to that for C_o(10) at the 95% confidence level.

In addition to the crimp-length interaction, two more two-factor interactions and one three-factor interaction have significant effects on E(10) at 90% confidence.

Three-factor interactions cannot be illustrated graphically in one diagram. Moreover, as the number of interacting variables increases, each point on a particular diagram represents an average of fewer data points, and is therefore less reliable. For this reason, the three-factor interaction found to be significant at 90% (shape x linear density x crimp) will not be considered.

The two other two-factor interactions (shape-length and linear density-shape) are presented in Figures 13 and 14. Explanations of all first-order and second-order effects will be given in the last part of this section.

B. Particle Size Analysis

In addition to efficiency and pressure drop characteristics, the particle size distribution of the dust in the outlet air stream is an important aspect of filtration performance. A Coulter* Counter was used to obtain distributions for the original fly ash (i.e., for a sample taken from the ash bin) and for the fractions that passed through the main filter. From these distributions it was possible to obtain the filter efficiency distribution, or the efficiency of the filter at each particle size level.

*Coulter Electronics, Inc., Hialeah, Fla.

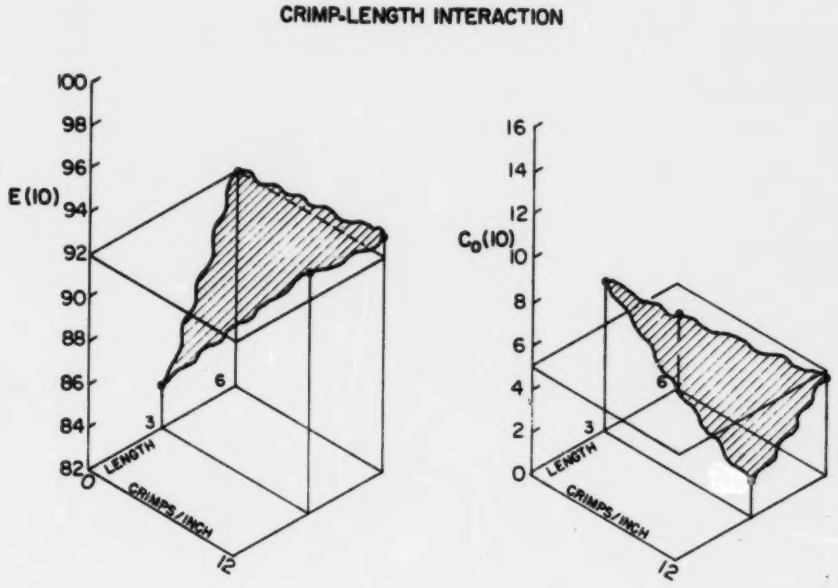

Fig. 12 Three-dimensional plots of the effect of crimp x length on E(10) and $C_o(10)$.

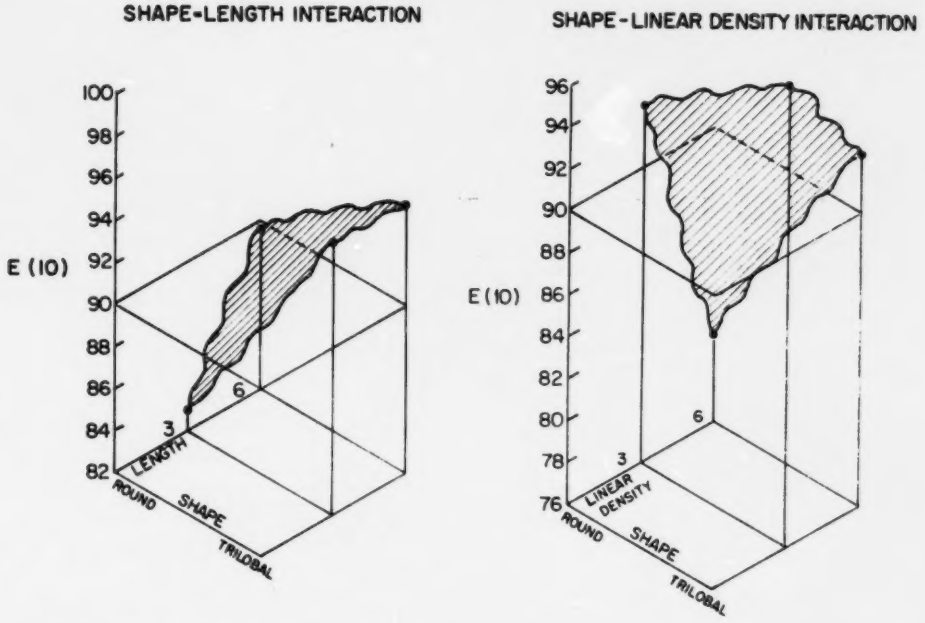

Fig. 13 Three-dimensional plot of the effect of shape x length on E(10).

Fig. 14 Three-dimensional plot of the effect of linear density x shape on E(10).

The efficiency distribution function E(d) was calculated from the expression

$$E(d) = 1 - \frac{[1-E(10)]f'(d)}{f(d)}$$

where E(10) is the overall efficiency (at the tenth cycle),
f'(d) is the weight fraction of passed particles at a particular diameter, and
f(d) is the weight fraction of fed particles at a particular diameter.

The diameter, d, ranged from a low value of 2.52μ to the maximum diameter, with each increment taken corresponding to a doubling of the volume of a spherical particle. Efficiency distributions have been plotted in Figures 15-22. Examination of the plots reveals that most of the improvement in efficiency occurs at the small particle end of the distribution.

A Yates analysis was performed using the tenth-cycle efficiency at the 2.5μ level as a response (see Table 4, last column). The results are included in Table 5 and show that removal of these smallest particles is improved by use of trilobal fibers of low linear density. Although the Yates analysis did not show crimp to be an important parameter in this case, it appears from Figures 15-22 that for the "A" and "C" series (short fibers), crimp brings a visible improvement in the fine particle removal.

Observation of the efficiency distribution curves also reveals a difference between the curves on the left and right hand side of each pair corresponding to smoother and rougher fibers respectively. In a paired comparison of these curves at the low end of the distribution, rough fibers were more efficient than smoother fibers in 11 cases, less efficient in 2 cases, and equally efficient in 3 cases. The Yates coefficient shows that average efficiencies for rough fibers in this region (i.e., 2.5μ) are 45% greater than that for smoother fibers, but only at the 60% confidence level. Considering that scanning electron micrographs (Figure 2) have shown only a small difference between smooth and rough fibers in this study, the above observations suggest that significant effects might be found with fibers exhibiting greater differences in roughness.

By contrast, the average improvement due to surface roughness on the overall efficiency E(10) for all particles from 40 to 2.5μ is only 2.8%. It seems, therefore, that surface roughness becomes more important as particle sizes become smaller.

Another interesting observation may be made from Figures 15-22. Curves for samples 1,2,5, and 6(A,B,C, and D) clearly reflect the higher efficiency due to lower deniers.

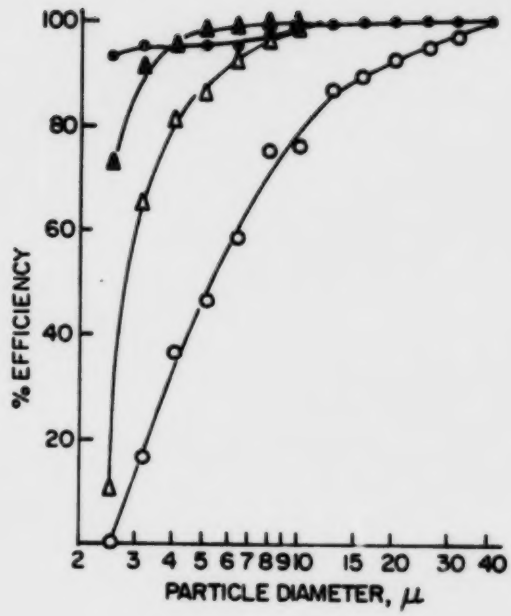

Fig. 15 Efficiency distributions for samples 1 A-D.

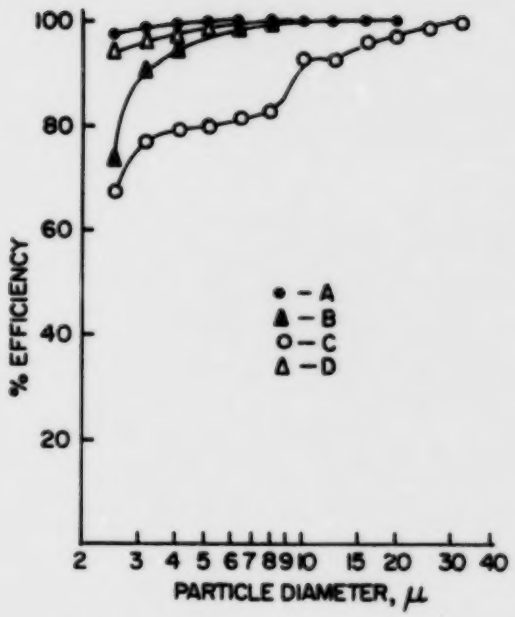

Fig. 16 Efficiency distributions for samples 2 A-D.

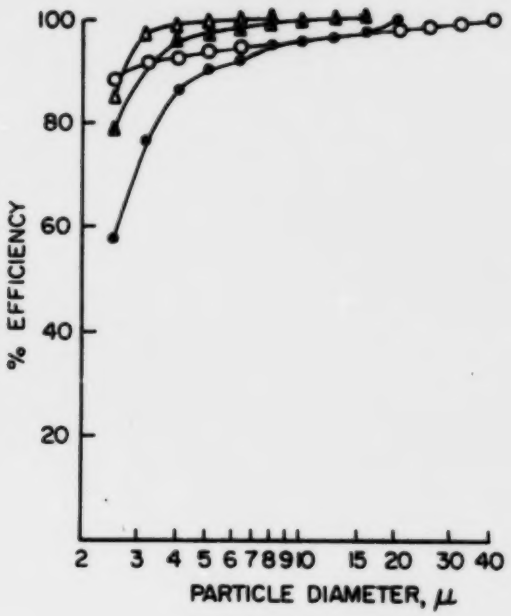

Fig. 17 Efficiency distributions for samples 5 A-D.

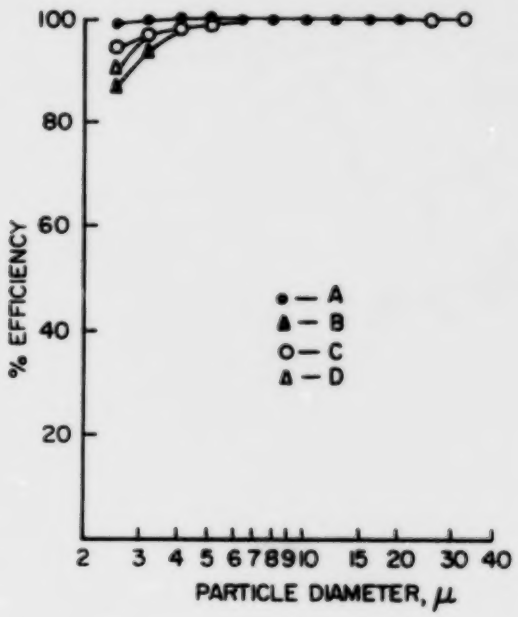

Fig. 18 Efficiency distributions for samples 6 A-D.

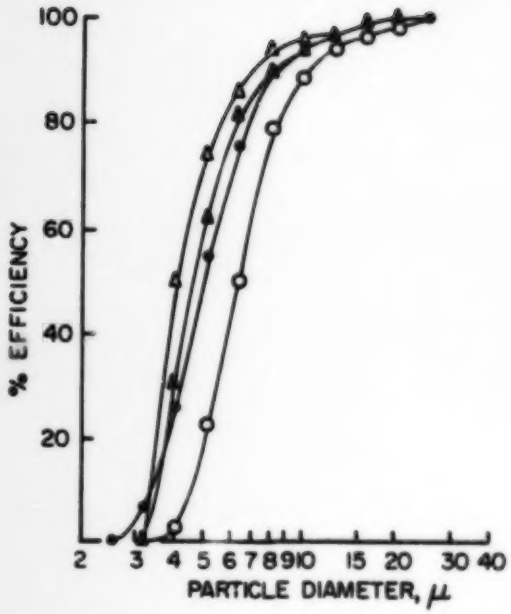

Fig. 19 Efficiency distributions for samples 3 A-D.

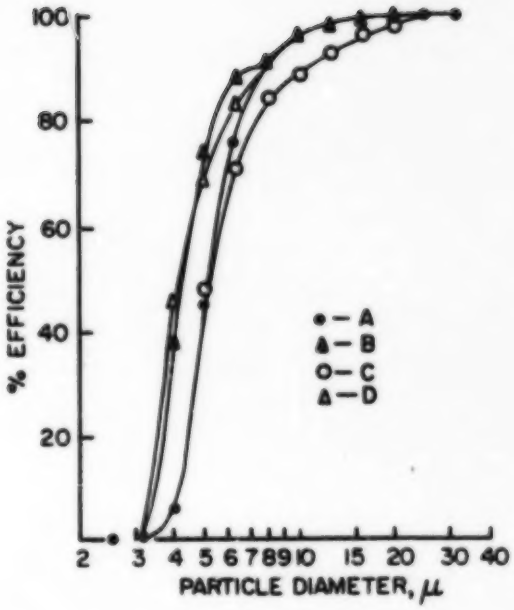

Fig. 20 Efficiency distributions for samples 4 A-D.

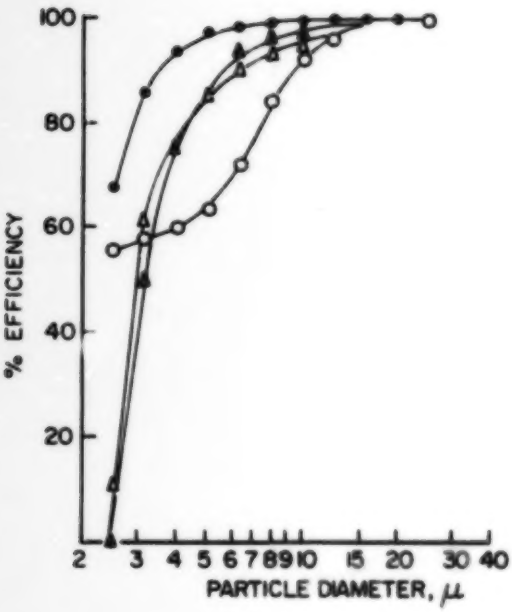

Fig. 21 Efficiency distributions for samples 7 A-D.

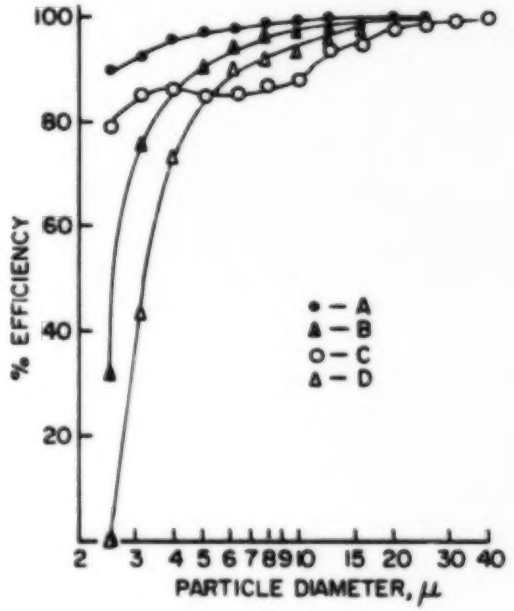

Fig. 22 Efficiency distributions for samples 8 A-D.

C. Physical Interpretation of the Results

Although theoretical expressions have not been derived for the relations between filtration responses and fiber parameters, qualitative explanations may be offered.

Surface Roughness - Micrographs presented in Figure 2 essentially explain the lack of effect on the major responses due to surface roughness since no great differences in roughness could be seen. The indication of improved efficiency at the small particle end of the distribution bears further investigation. It is possible that a relationship exists between the size of surface asperities and the size of particles to be captured.

Linear Density - Two explanations can be advanced. First, the projected area of a constant mass of fibers is inversely proportional to the square root of the linear density. It follows that with fibers of lower linear density, the probability of impact is increased. The second effect of decreasing linear density at constant fiber mass is an increase in the number of fibers. This in turn reduces the interfiber distances and facilitates "bridging." Similarly, the increased projected area and decreased pore size would be expected to produce higher drag characteristics.

Cross-Sectional Shape - A similar argument applies to the case of trilobal fibers. The 3-denier trilobal fibers used in this study have a 25% greater projected area than the 3-denier round fibers. The probability of impact increases proportionally. It is difficult to explain why the greater projected area of trilobal fibers does not cause increased drag. The increased projected area alone appears not to cause as much of an increase in drag as would an increase in the number of fibers due to a decrease in linear density, which also decreases the average interfiber spacing. It can be seen in Figure 23 which shows views of the downstream side of the fiber, that there appears to be a trapping mechanism peculiar to trilobal fibers, where particles lodge in the concave region of the fiber.

Crimp - This parameter improves both efficiency and drag characteristics. The reason for the reduced drag and higher efficiency with crimped fibers may be found in Figure 23B. It can be seen that straight fibers seem to form groups of two or more where the fibers run close together for a considerable length. The space between them becomes clogged with filtered particles, and the group then acts as a single wide flat fiber with a higher resistance to air flow. Efficiency decreases because of the larger spaces between these groups. None of these groups is visible in the photograph of crimped fibers (Figure 23A) which maintain an open structure.

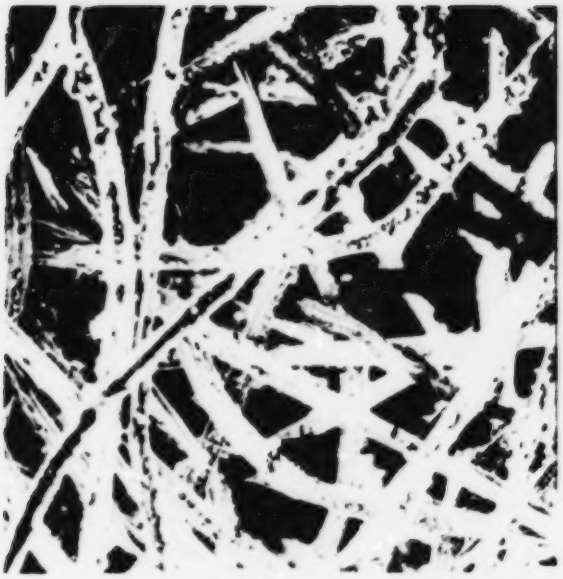

a) Sample 6A (3-den, trilobal, crimped)

b) Sample 4C (6-den, round, uncrimped)

Fig. 23 Scanning electron micrographs of filters 4C and 6A (150X)

Length - The reason for the improvement in efficiency with greater fiber length is not obvious, but becomes more understandable as interactions at the 90% level are examined.

Interpretation of two-factor interactions is difficult. Interactions are likely to be a result of structural changes in the fabric due to variables, and not simply inherent in the variables themselves. Consequently, they must remain subject to conjecture, with few exceptions (as in the case where some structure difference could be observed between micrographs of filters made from crimped and uncrimped fibers). With this caution in mind, the following tentative explanations are offered:

Crimp-Length Interaction - This interaction is most significant since its effect on E(10) is at the 90% level and on C_o(10) is at the 95% level. Two physical interpretations appear to be involved. First, it is proposed that in the carding process, the crimp was removed from the longer fibers by a stretching action. Both 3-in. and 6-in. fibers were processed on the same card and it is likely that this unit, not being optimized for the longer fibers, subjected the latter to severe elongation and removed much of the crimp. This explains the lack of effect of crimp in long fibers and why short crimped fibers were more efficient (lower C_o) than long crimped fibers. This does not explain the large difference between short and long uncrimped fibers. A second physical interpretation must also be offered. While crimp does indeed "open" the fiber bundles and thus improves efficiency by creating a more uniform distribution of fibers (and lower drag), it also appears that staple length may have the same effect as crimp. Having a better chance of being caught by the card, long staple fibers result in a more even distribution of fibers even in the absence of crimp. This explains the occurrence of lower efficiency in the case of short uncrimped fibers which have the advantage of neither length nor crimp. The same effect is mirrored in the crimp-length interaction found in the outlet concentration response, which shows high values only with short uncrimped fibers.

Shape-Length Interaction - A similar mechanism appears to be in effect for the cross-sectional shape - fiber length interaction. A trilobal shape has the same effect as crimp in promoting fiber separation and thus uniform distribution. Accordingly, efficiency is poorer for short round fibers than for the other three combinations. The improvement in E(10) due to greater length for both round and uncrimped fibers causes an overall increase in the average E(10) due to length. This explains the appearance of fiber length at the 90% confidence level.

Linear Density-Shape Interaction - This interaction reflects merely that in going from round to trilobal fibers, efficiency increases less for 3-denier than for 6-denier fibers. This

occurs because 3-denier filters have a high efficiency even with round fibers, and have therefore a lesser possibility of rising further. It is possible that if efficiency were plotted on a logarithmic scale, this interaction would not appear.

The above observations lead to the conclusions that interactions arise from differences in fiber arrangement in the nonwoven fabric. It follows that a different set of interactions might well be observed if the filter fabrics were fabricated by a different process, e.g., a different card or an air-laid random-webber.

SECTION VIII

EDP SCANNING MICROSCOPE

In the previous section it has been shown that significant interactions may occur as a result of differences in fiber arrangement within the nonwoven structure. A preliminary investigation of variations in fiber distribution from web to web was made using an EDP Scanning Microscope.* This instrument provides an optical density contour map of a specimen as it is spirally scanned from the center outward by a transmitted beam of light 200 microns in diameter. The light transmitted by the specimen passes to a photocell and is converted into an electrical signal proportional to the amount of light transmitted. This signal charges the stylus of a facsimile printer which is mechanically coupled to the scanning stage, thereby producing the contour map as the instrument is operating. The contours may consist of a maximum of sixteen distinguishable shades of darkness. The density distribution can therefore be quantitatively mapped. The radial velocity of the stylus is greater than that of the light beam by an adjustable factor of 1 to 50. The contour map is therefore a magnified image. Figures 24A and B are 5.5X magnifications of samples #4C and #4A. The density of these samples is 0.06 g/cm^3 and their weight is 0.8 oz/yd^2. As can be seen in Table 2 these samples differ in crimp level only. In Figure 24A, the uncrimped sample shows a large number of random lines of width equivalent to 4 to 6 fiber diameters. These lines represent fiber bundles. No such lines are visible in Figure 24B depicting the crimped sample. These results essentially verify the assumptions made in the previous section with regard to the effect of crimp.

Denser and heavier filter webs of these same two samples were also scanned. Figures 24C and D show the uncrimped sample and the crimped sample, respectively, at 5.5X magnification. The density of these webs is 0.14 g/cm^3 and their weight is 6.4 oz/yd^2. Light intensity was increased to compensate for greater density and weight. Individual fiber bundles are no longer visible in the uncrimped sample. However, the dark and light contours are seen to be less evenly distributed and larger than those for the crimped sample.

These preliminary results obtained with the EDP Scanning Microscope indicate that it is a promising method for further investigation of fiber distributions within the web structure. The time available in the period covered by this report was not sufficient for a complete study using these techniques.

---

*Manufactured by Photometrics, Inc., Lexington, Mass.

Uncrimped Crimped

Fig. 24 Optical density contour maps of filter samples (5.5X):

A. Low density sample #4C
B. Low density sample #4A
C. High density sample #4C
D. High density sample #4A

SECTION IX

EPITROPIC FIBERS

A. Surface Roughness

In the principal study of the present project, one of the variables was fiber surface roughness. Fibers with different surface roughness were obtained by addition of two levels of TiO_2 (0.1% and 2.0%). However, subsequent microscopical examination showed that even at the 2.0% TiO_2 level the degree of roughness was not pronounced. This was consistent with the observation that, in general, no significant effects of roughness on filtration performance were found with these samples. However, at the small end of the particle size distribution, some increase in efficiency was apparent from visual examination of efficiency distribution curves and also by a score-card method. This suggested that significant effects might be found using fibers with higher degrees of roughness. These could be obtained by addition of greater amounts of TiO_2, but it is known that increases in filler content would lead to problems in fiber formation and to deterioration of fiber tensile properties.

Epitropic (surface-modified) fibers are a recent development of ICI Fibres Ltd., (England)[13], and represent a means of introducing high levels of solid additives without encountering the above difficulties. Using an as yet unpublished technique, a central fiber core is encased in an outer layer of lower melting polymer containing a very high percentage of filler. Figures 25 and 26 show micrographs of such a fiber and its cross section; the substantial surface concentration of the filler is evident.

Since such fibers might be suitable for a further study of roughness effects on filtration, a quantity was obtained in the form of 3-denier, 3-inch, uncrimped staple. The core polymer and low melting point outer polymer was polyester, and the filler was carbon black particles smaller than 5μ. The specific gravity of these fibers is 0.30 g/cc, which is very close to that of polyester fibers.

Card webs were then made from a 50/50 blend of epitropic fibers and polyester fibers selected from the main experiment. The particular fiber sample chosen (#1-C) was 3-den., 3-in., and uncrimped, and therefore similar to the epitropic fibers in all properties except roughness. As a control, a card web of 100% polyester (sample #1-C) was also made.

Filter fabrics were prepared from these webs according to the procedure described in Section VI. The properties of these fabrics are given in Table 6.

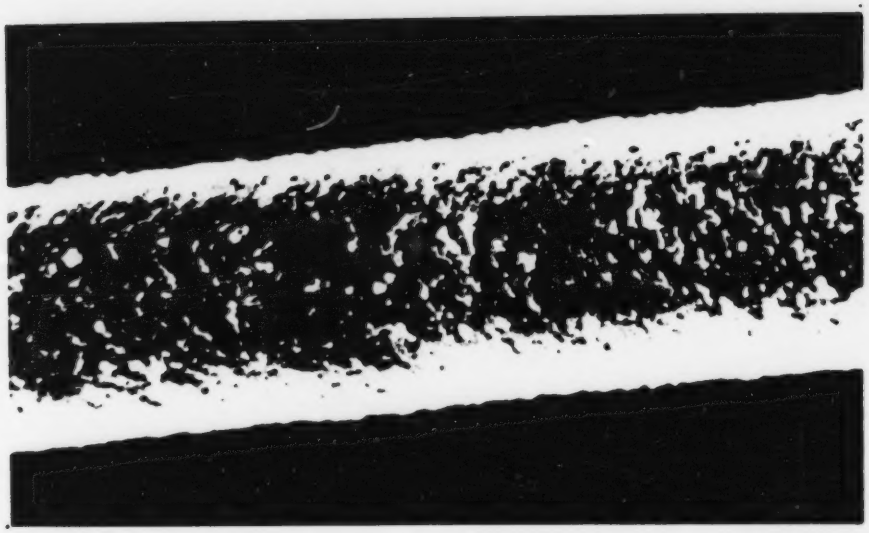

Fig. 25 Micrograph of epitropic fiber surface (from Ellis, V. S., Reference 13).

Fig. 26 Micrograph of epitropic fiber cross section (from Ellis, V. S., Reference 13).

Experiments were conducted with a finer fly ash (<10 μm) than previously used. It was obtained by cyclone separation downstream from the feeder. The 50/50 epitropic/polyester sample and the 100% polyester sample were measured for first-cycle efficiency E(1). The pressure drop across both samples was too low to be measured, since no appreciable cake buildup occurred. Two replicate runs for each sample were used to determine particle size distribution resulting in the efficiency distribution curves shown in Figure 27. The higher efficiency for the polyester sample is reflected in the efficiency distribution curves especially at smaller particle sizes (4μ and below). The overall average E(1) was 94.3 for the polyester sample and 89.8 for the epitropic/polyester blend. This result was unexpected since the fiber with increased surface roughness was apparently less efficient than the smooth fiber.

An explanation of this anomalous result may lie in the conductivity of the carbon black on the surface of the epitropic fibers. If there is a tendency for charge buildup on a filter while it is operating, with the epitropic fibers such charges probably would leak away to the metallic filter holder. This would act against any electrostatic aggregation of particles with its associated increase in collection efficiency. However, the 100% polyester fibers, being essentially nonconductive, would retain most of the induced charges which would then be available to assist in the aggregation process. This electrostatic effect on efficiency is presumably greater in this case than any opposite effect due to surface roughness.

B. Electrostatic Effects

The conductivity of epitropic fibers is considerably higher than that of polyester fibers. The resistance of a 50/50 epitropic fiber/polyester nonwoven was found to be about 10^4 ohms while that of a polyester nonwoven was about 10^{10} ohms. It was decided to measure the effect of this property on filtration efficiency as voltages are applied to the filter fabric. The filtration apparatus was modified as shown in Figure 28. The aluminum filter holder was insulated from the filter chamber wall by a rubber ring. The ducts on either side of the filter holder were converted to plastic tubing for further insulation. Connections were made from a high voltage power supply to the filter holder and from the filter chamber wall to ground. With the power supplies available, either positive or negative charges could be generated on the filter holder and filter in the range of -2 Kv to + 30 Kv. The upper voltage level for positive polarity was limited to 10 Kv since audible discharging occurred above this level.

Table 6

PHYSICAL PROPERTIES OF EPITROPIC/POLYESTER FILTERS

		Wt. (oz/yd^2)	Dens. (g/cm^3)	% Latex Add-on
50%/50% Epitropic/ Polyester	1	5.49	0.148	4.87
	2	5.63	0.150	4.65
100% Polyester	1	5.54	0.148	3.36
	2	5.52	0.152	4.13

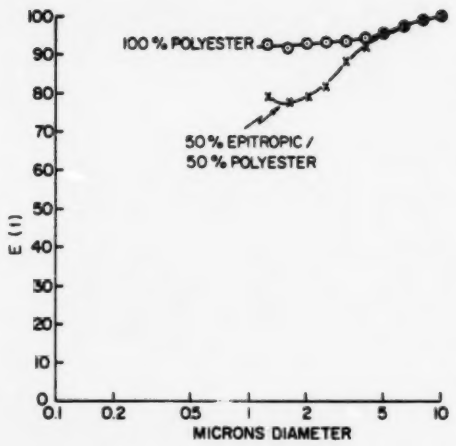

Fig. 27 Efficiency distribution curves for 100% polyester and for 50% epitropic/50% polyester filter samples.

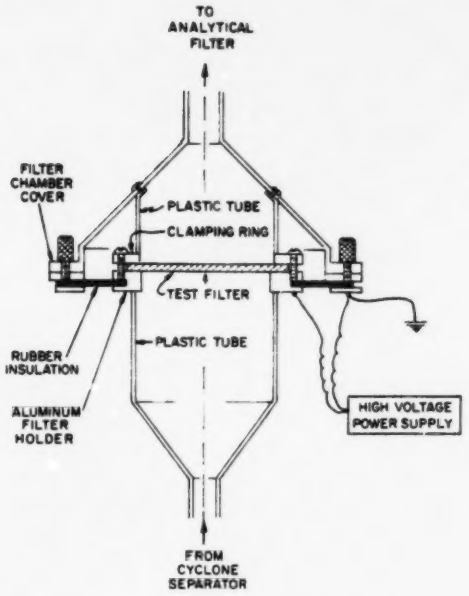

Fig. 28 Diagram of filtration apparatus modification for electrification trials.

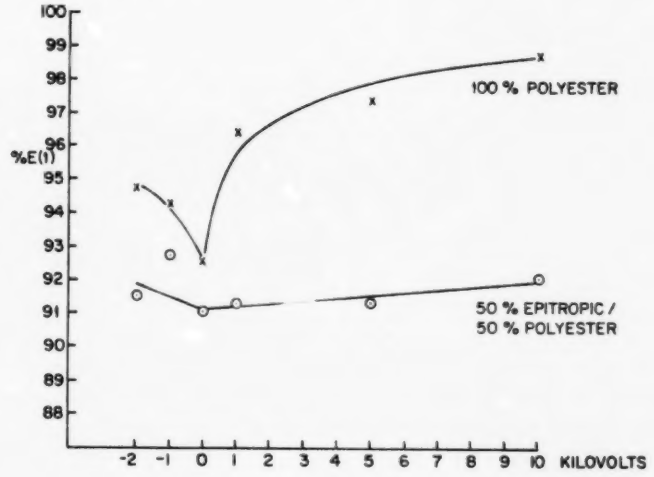

Fig. 29 Effect on E(1) of high voltage applied to 100% polyester and to 50% epitropic/50% polyester filters.

An epitropic/polyester sample and a polyester control sample were then subjected to high voltage while filtration was going on under the same conditions as before. Only one specimen was used for each sample so that construction variability would be eliminated as voltage was varied. Since the deposit of fly ash after each filtration was small, it was possible to vacuum-clean almost all deposit from the samples after each filtration. Vacuum cleaning was conducted through a metallic screen to avoid damage to the filter. To further reduce the possible effect of the residual dust, voltages of -2, -1, 0, + 5, and + 10 kilovolts) were applied to both samples and two or three repeat measurements were taken at each voltage level, all in random order. The averages of first cycle efficiency results have been plotted in Figure 29.

Filtration efficiencies for the two samples, while about the same under zero charge conditions, become significantly different when charges were applied. The epitropic/polyester filter was affected little or not at all by charging either positively or negatively. The polyester filter, however, showed a definite increase in E(1) as the positive voltage increased. The increase in E(1) from 92.5 at 0 KV to 98.8 at + 10 KV was equivalent to a reduction in the outlet concentration of almost 90%. With negative voltage, the polyester sample also showed a comparable increase to the limit of -2 KV.

The improvement in efficiency obtained by charging the 100% polyester samples is due to the potential gradient developed across the filter. It may be assumed that small leakage currents allow a lowering of potential in the central portion of the filter; when the fibers are conductive no such potential gradient may be established. The gradient may be increased with polyester fibers by grounding the center of the filter. Figure 30 shows first cycle efficiency for a needle-punched nonwoven fabric. The improvement following the application of a voltage to the outer edge is significant. If the center of the sample is grounded there is a large further increase in efficiency. Since the radius of the filter was about 5 cm, the maximum potential gradient established (at 10 KV) was about 2 KV/cm.

The principle has been described previously by Rivers [14]. It appears not to have found application in baghouse filter fabrics, but a study of the savings in energy that could be derived from use of low drag filters rendered more efficient by application of electric voltages would seem worthwhile.

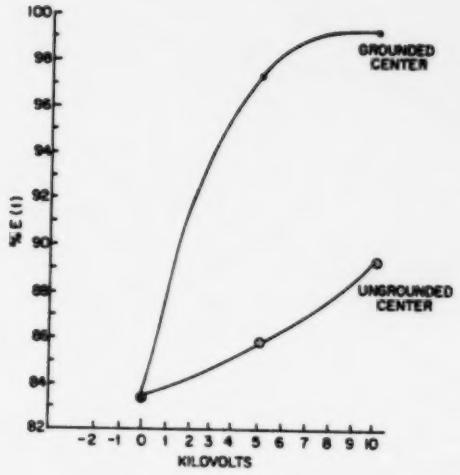

Fig. 30 Effect on E(1) of high voltage applied to 100% polyester (needled) with and without grounding center of sample.

SECTION X

REFERENCES

1. Turner, J. H., "Performance of Nonwoven Nylon Filter Bags," Paper No. 73-300, APCA Annual Meeting, June 1973.

2. Ranz, W. E., "The Impaction of Aerosol Particles on Cylindrical and Spherical Collectors." Technical Report No. 3, Contract No. AT(30-3)20 SO 1004, (1951).

3. Davies, C. H., "Separation of Airborne Dust and Particles," Institute Mechanical Engineers (London), Proceedings (B) 1B, No. 5, pp 185-213, (1952).

4. LaMer, V. K., "Studies on Filtration of Monodisperse Aerosols." U. S. Atomic Energy Commission, Report NYO 512, Contract No. AT(30-1)-651, (1951).

5. Ranz, W. E., "Principles of Inertial Impaction." Engineering Research Bulletin B-66, College of Engineering and Architecture, Pennsylvania State University, (1956).

6. Ranz, W. E. and Wong, J. B., "Impaction of Dust and Smoke Particles on Surface and Body Collector." Industrial and Engineering Chemistry 44, pp 1371-1381, (1952).

7. Zimon, A. D. and Lazarev, K. A., Kollidnyi Zhurnal 31, No. 2, pp 214-219, March 1969.

8. Leva, M., "Fluid Flow Through Packed and Fluidized Systems." Bureau of Mines Bulletin 504, U. S. Government Printing Office, (1951).

9. Dahneke, B., "Capture of Aerosol Particles by Surfaces," Journal of Colloid & Interface Science 37, No. 2, pp 342-353, (1971).

10. Durham, J. R. and Harrington, R. W., AICHE 63rd Annual Meeting, Chicago, Illinois, November 1970.

11. Rodebush, W. H., et al, Report No. 2050, PB 32203, November 24, 1932.

12. Daniel, C., "Use of Half-Normal Plots in Interpreting Factorial Two-Level Experiments." Technometrics 1, No. 4, pp 311-341, (1959).

13. Ellis, V. S., "Epitropics-Third Generation Conductive Fibers," Textile Manufacturer 101, No. 1193, pp 19-23 July 1974.

14. Rivers, R. D., "Operating Principles of Non-Ionizing Electrostatic Air Filters," ASHRAE Journal, pp 37-40, February 1962.

SECTION XI

GLOSSARY

Card - A textile processing machine which separates fibers from each other, lays them parallel, and forms them into a thin web.

Crimp - (1) The waviness of a textile fiber
(2) An individual wave in a textile fiber

Denier - A unit of linear density corresponding to the weight in grams of 9000 meters of a filament or yarn.

Drag - The pressure drop across a filter divided by the face velocity (volumetric flow rate normalized for filter area).

Effective Drag - The drag after the filter has been established and is at the point in the filtration cycle where a cake has been established and the change in pressure drop with time becomes a straight line function.

Efficiency - The percentage of the total weight of dust impinging on a filter that is collected by the filter.

Epitropic Fiber - A fiber whose surface contains embedded particles which modify one or more of the fiber properties. (From the Greek epi meaning upon and tropaios to change).

Fly Ash - A product of coal burning consisting of spherical particles ranging in diameter from several hundred to below one micron.

Interaction - A combination of two or more independent variables (a second or higher order term) that acts as a single variable.

Yates Algorithm - A statistical method for calculating the coefficients in the linear model representing any two-level factorial experimental design.

Outlet Concentration - The weight of dust per volume of air that passes through a filter.

Specific Cake Resistance - The change in drag per mass of dust cake per unit filter area.

Staple - Fiber, cut into short pieces, that can be processed on a card.

Terminal Drag - The drag at the end of a filtration cycle just before cleaning.

Trilobal - A fiber cross-sectional shape with three rounded projections.

SECTION XII

NOMENCLATURE

A	area of filter
C_o	outlet concentration
$C_o(10)$	outlet concentration of tenth cycle
C_i, C_{ij}, C_{ijl} ...	Yates coefficients
d	diameter of particle
E(1)	efficiency at the first cycle
E(10)	efficiency at the tenth cycle
E(10)(2.5μ)	efficiency at the tenth cycle for particles 2.5μ diameter
E(d)	efficiency for particles of diameter d
f(d)	weight fraction of passed particles at a particular diameter
f'(d)	weight fraction of fed particles at a particular diameter
k	number of variables in Yates analysis
K	specific cake resistance
m_c	mass of dust captured
m_p	mass of dust passed
n	rank number of Yates coefficient
N	total number of Yates coefficients
ΔP_e	effective pressure drop
ΔP_f	final pressure drop
Q_c	volumetric flow of air through the filter
S	drag

t_c	time period for one cycle
V	face velocity
W	mass of dust per unit area of filter
X_i, X_{ij}, $X_{ij\ell}$ ...	Yates variables
Y_e	estimated value of response in Yates analysis